IEEE Access
Multidisciplinary ⋮ Rapid Review ⋮ Open Access Journal

Received June 19, 2020, accepted July 6, 2020, date of publication July 10, 2020, date of current version July 28, 2020.

Digital Object Identifier 10.1109/ACCESS.2020.3008569

Hot Water Deicing Method for Insulators Part 2: Analysis of Ice Melting Process, Deicing Efficiency and Safety Distance

ZHANG ZHIJIN[1], YANG SHENGHUAN[1], JIANG XINGLIANG[1], (Senior Member, IEEE), MA XIAOHONG[2], HUANG HUAN[2], PANG GUOHUI[1], JI YAQING[1], AND DONG KAI[1]

[1]School of Electrical Engineering, Chongqing University, Chongqing 400044, China
[2]Electric Power Research Institute, Guizhou Power Grid Company Ltd., Guiyang 550002, China

Corresponding author: Zhang Zhijin (zhangzhijing@cqu.edu.cn)

This work was supported in part by the Guizhou Science and Technology Plan Project under Grant [2020]4Y051.

ABSTRACT In this paper, the heat balance integral method was employed to solve the internal temperature of ice layer and the position of melting interface by stages, due to its main advantage of converting the governing partial differential equation to an ordinary differential one, which can effectively reduce numerical efforts. Then the deicing time of hot water for insulator was calculated and analyzed. Taking LXY-120 insulator as the verification object, after natural icing at Xuefeng mountain natural icing test base, the validation experiments of deicing time were carried out in the natural environment. The initial water temperature and outlet pressure were optimized for deicing efficiency. Finally, the leakage current of water jet was measured. The research results indicate that the deicing rate increases and the energy consumption gradually decreases as the initial temperature of hot water increases. As the outlet pressure increases, the deicing rate increases. For the deicing condition of 1.2 mm nozzle, ambient temperature of −1 °C, wind speed of 3 m/s, ice weight of 2 kg/piece and deicing distance of 2 m, when the initial temperature of hot water and outlet pressure are 85.21 °C and 3.35 MPa respectively, the comprehensive deicing efficiency is the highest. The leakage current through water jet decreases with the increasing distance. The leakage current increases with the increase of water conductivity and outlet pressure. Hot water deicing for insulator in 110 kV system can be carried out according to the safety distance of the existing regulation.

INDEX TERMS Insulator, melting process, deicing efficiency optimization, safety distance.

I. INTRODUCTION

Insulator plays an important role of electrical insulation and mechanical support in the transmission line, and its icing may cause ice flashover which would lead to the interruption of power supply [1]–[6]. Hot water deicing for insulators belongs to the melting process with phase change. The theoretical solution methods of phase change problem can be divided into exact solution and approximate solution. The former method is only applicable to some simple models and boundary conditions, and it is almost impossible to deal with the problem of insulator deicing. Approximate solutions mainly include quasi-steady state method, thermal resistance method and polynomial heat balance integral method [7]–[12]. The main advantage of the heat balance integral method is the transformation of the governing equation from a partial differential form to an ordinary differential one, which allows satisfactory results with less numerical efforts [7], [9]. It is a typical method to solve the problem of heat transfer with phase change and applicable for the phase change problem with the conditions of semi-infinite and finite thickness in the rectangular [11], [12] and spherical [13], [14] coordinates. In literature [11], [12], the polynomial heat balance integral method is used to solve the temperature field in melting process of ice layer with semi-infinite and finite thickness, respectively.

Regarding the influencing factors of the efficiency of various deicing methods, the efficiency of hot air deicing in literature [15] is determined by the deicing time and energy consumption together. Comprehensive deicing efficiency is highest at the hot air speed of 13.87 m/s and temperature of 192.27 °C. Literature [16], [17] pointed out that the laser power density and the temperature of infrared transmitter are important factors that affect the efficiency of laser and

The associate editor coordinating the review of this manuscript and approving it for publication was Jason Gu.

infrared deicing respectively. In the aspect of water jet deicing, literature [18], [19] studied the deicing method using water jet of low temperature (between 0 °C and 4 °C). The influence of jet pressure, distance and ice temperature on the deicing efficiency was studied preliminarily. It pointed out that the deicing efficiency can be raised by increasing the ice layer temperature [18]. The deicing experiment of post insulator was carried out in literature [20] on the condition of hot water temperature of 50 °C, hot water speed of 15 m/s, ice thickness of 5 mm and the deicing distance of 50 cm. The experiment results indicate that removing the ice with thickness of 5 mm takes 1.71 min and consumes hot water of 32.43 L. Besides, it was found that the deicing time and energy consumption of hot water deicing method are related to the hot water temperature and jet velocity, and the deicing time and energy consumption are superior to the hot wind and electric heating deicing method [20]. Road deicing using hot water jet was studied in literature [21]–[23], in which the deicing depth is taken as the measurement and the effects of outlet pressure and hot water temperature are mainly studied. It was obtained that under the condition of nozzle diameter of 1.75 mm and target distance of 45 mm, the deicing effect is best when the jet pressure and temperature are 0.46 MPa and 89-93 °C respectively [21], [22]. From the above literature, it can be summarized that the temperature and outlet pressure (or speed) of the deicing medium are the key factors affecting the deicing time and energy consumption, thus affecting the comprehensive deicing efficiency.

The insulation of water jet is the key factor to ensure the safety of live operation. According to the standard [24], the leakage current through the water column during hot washing for electric power apparatus should not exceed 1 mA. The leakage current of water jet was measured in literature [25], and the minimum water column length of live washing working was proposed under different nozzle diameter, water resistivity and pressure in 500 kV system.

This article is the second in the series. In the first article, the propagation and temperature spatial distribution characteristics of hot water jet in the air were studied. The research results are summarized as follows: the effect of increasing the initial temperature of hot water to increase water jet temperature decreases with the increase of distance. As distance increases, the temperature of water jet gradually decreases. Increasing outlet pressure causes the water jet temperature to drop slightly. When the ambient temperature and the wind speed decrease or increase by the same value, wind speed reduces the temperature of water jet to a greater degree than the ambient temperature. Increasing the nozzle diameter can effectively increase the water jet temperature at the same distance.

This paper focuses on the deicing process on the insulator surface under hot water, and the deicing efficiency and safety distance of hot water deicing technology are discussed and analyzed. The research results provide theoretical support for revealing the influencing factors and mechanism of hot water deicing and the selection of deicing equipment parameters.

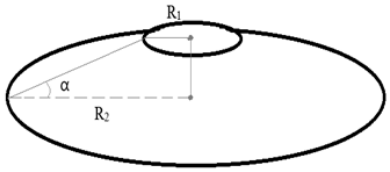

FIGURE 1. Simplified schematic diagram of insulator shed.

II. CALCULATION MODEL OF HOT WATER DEICING TIME FOR INSULATORS

A. PHYSICAL CALCULATION MODEL FOR DEICING TIME OF HOT WATER

It is assumed that the surface of the insulator is covered with ice uniformly. During the deicing process, after hot water is jetted onto the insulator surface, the geometry of insulator shed causes that part of the water spatters around and some drips along the shed edge. In general, the heat transfer area does not exceed the area of a single shed. Therefore, in the following calculation model, it is approximated that hot water only acts on one insulator after being sprayed onto the surface of the insulator. The insulator shed is approximated as the frustum of a cone, as shown in Fig. 1, and the surface area of the insulator shed is

$$S = \frac{\pi}{\cos\alpha}\left(R_2^2 - R_1^2\right) \tag{1}$$

where α is the inclination angle of the insulator surface, R_1 and R_2 are the radius of the metal fitting and the outer edge radius of the shed, respectively.

The number of insulators is n, the thickness of ice layer is H, and the density of ice is ρ. The total mass of ice coating is

$$\mathrm{m_{ice}} = n\rho SH \tag{2}$$

When the hot water flows past the surface of ice layer, the heat exchange between the hot water and ice layer is called convective heat transfer. The heat exchange amount of convective heat transfer can be calculated by the Newtonian cooling formula [26]. For the unit area, the heat q (W/m^2) transferred from hot water to ice layer during unit time is

$$q = h(T_\mathrm{w} - T_\mathrm{ice}) \tag{3}$$

where h is the convective heat transfer coefficient on the ice layer surface, W/(m^2 ·°C); T_w is the temperature of the hot water reaching the ice layer, °C; T_ice is the ice layer temperature, °C.

Besides, the convective heat transfer coefficient h that hot water flows past the solid, the average Nusselt number N_u in the heat transfer area, the thermal conductivity of hot water k and the feature size of heat transfer L satisfy the following relationship [26]:

$$h = kN_\mathrm{u}/L \tag{4}$$

where N_u is the ratio of convective heat transfer resistance of fluid layer to thermal conduction resistance, indicating the intensity of convective heat transfer. L is related to the radial width of water column and the effective heat transfer area of hot water is approximately regarded as a circular area with

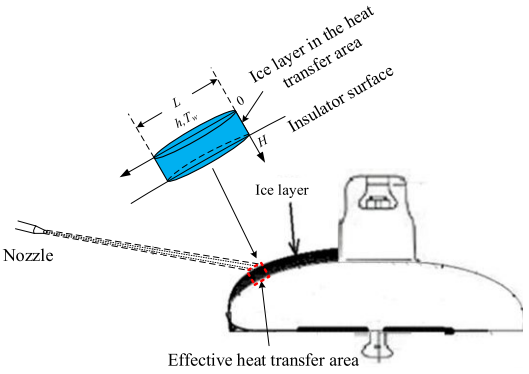

FIGURE 2. Schematic diagram of the effective heat transfer area of the ice layer (thickness *H*).

the width of water column as its diameter, and the feature size of heat transfer is the diameter. Therefore, the convective heat transfer coefficient can be obtained by calculating the average Nusselt number.

According to the literature [27], [28] on the research of the convection heat transfer process on flat plate, the average Nusselt number N_u is

$$Nu = \begin{cases} 0.664Re^{1/2}\,\mathrm{Pr}^{1/3} & (Re \le 5\times 10^5) \\ \left(0.037Re^{4/5} - 871\right)\mathrm{Pr}^{1/3} & (Re > 5\times 10^5) \end{cases} \quad (5)$$

where Re is the Reynolds number, which characterizes whether the fluid flow is laminar or turbulent. Pr is the Prandtl number, which is related to the water temperature and can be obtained from the table of hydrothermal physical properties.

The Reynolds number that the hot water flows on the surface of ice layer is

$$\mathrm{Re} = LV_w/\nu \quad (6)$$

where ν is the kinematic viscosity of water, m^2/s, and the kinematic viscosity at different water temperature can be obtained from the hydrothermal physical property table; V_w is the hot water velocity, m/s.

Because high-speed hot water is continuously jetted onto the surface of ice layer and the insulator shed is inclined, the hot water newly reaching the ice layer surface would wash away the melted water and the low-temperature water produced after heat exchange. Therefore, the simplification is made that the melted part is removed immediately upon formation [29], [30], which means the temperature of hot water on the ice layer surface can be approximately regarded as constant. This study belongs to the range of convective phase change under the third type of boundary condition (that is, the temperature of the heat exchange fluid is unchanged).

The effective heat transfer area of hot water jet on the insulator surface is small. The ice melting in the area where the hot water contacts the ice layer is regarded as the convection melting process with limited thickness in the effective heat transfer area. Taking the ice layer in this area as a calculation unit and ignoring the heat diffusion outside the effective heat transfer area, its transfer in the thickness direction of the ice layer is considered. The calculation model is shown in Fig. 2.

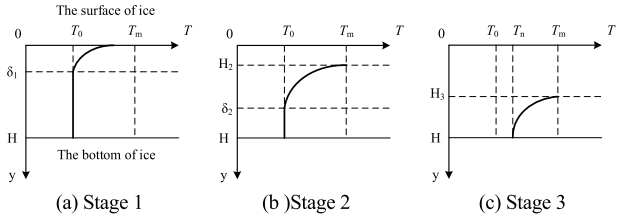

FIGURE 3. Temperature distribution inside the ice layer along the thickness direction at different melting stages.

The initial temperature of the ice layer is the same as the ambient temperature, T_0, the melting point is T_m, the thermal conductivity of ice is λ, the latent heat of melting is L_1, and the thermal diffusivity is a.

The melting process is divided into three stages according to the changes of temperature penetration depth inside the ice layer and melting interface, as shown in Fig. 3. The first stage is from the beginning of the heat transfer process when hot water reaches the ice layer ($t = 0$ s) until the temperature of the top of the ice layer rises to $T_m(t = t_1)$. The temperature penetration depth in this stage is $\delta_1(t)$. The second stage takes t_1 as the starting point and that the temperature at the bottom of ice layer begins to rise ($t = t_2$) as the end point. The temperature penetration depth in this stage is $\delta_2(t)$, the melting interface position is $H_2(t)$ and $\delta_2(t_2) = H$. The third stage starts from $t = t_2$ until the melting interface reaches H. The position of the melting interface is $H_3(t)$ and the temperature at the bottom of the ice layer is $T_n(t)$ in this stage.

The internal temperature of ice layer is solved by the cubic polynomial heat balance integral method, which approximates the ice layer temperature as a cubic function of position y and time t [7], [8], [12], and the temperature distribution equation is

$$T(y,t) = A + B(\delta(t) - y) + C(\delta(t) - y)^3 \quad (7)$$

where A, B, C and $\delta(t)$ can be solved by the solution conditions at each stage.

(a) Stage 1: Heat transfer begins until the temperature of the top of the ice layer rises to the melting point

During this stage, there is no phase change in the ice layer. In the range of penetration depth $[0, \delta_1(t)]$, the temperature increases with the increase of y. The ice layer temperature outside the penetration range is T_0. It is assumed that, at the position of penetration depth $\delta_1(t)$, the temperature rises smoothly from T_0 [8]–[12]. In this stage, the differential equation of heat conduction inside the ice layer and the definite solution conditions are:

$$\frac{\partial T}{\partial t} = a\frac{\partial^2 T}{\partial y^2} \quad 0 < t \le t_1\ 0 \le y \le \delta_1(t) \quad (8)$$

$$T = T_0, \quad \frac{\partial T}{\partial y} = 0 y = \delta_1(t) \quad (9)$$

$$-\lambda\frac{\partial T}{\partial y} = h\left(T_w - T(y,t)\right) y = 0 \quad (10)$$

Substituting equations (9) and (10) into equation (7), it is obtained that $A = T_0$, $B = 0$, $C = h(T_w - T_0)/[\delta_1(t)^2(3\lambda + h\delta_1(t))]$. Then the temperature distribution

in the ice layer along the thickness y direction can be expressed as

$$T(y,t) = T_0 + \frac{h(T_w - T_0)}{\delta_1(t)^2(3\lambda + h\delta_1(t))}(\delta_1(t) - y)^3 \quad (11)$$

Integrating equation (8) at $y \in [0, \delta_1(t)]$, the equation about $\delta_1(t)$ can be obtained as follows

$$\frac{d\delta_1(t)}{dt} = \frac{12a(3\lambda + h\delta_1(t))}{6\delta_1(t) + \delta_1(t)^2 h} \quad (12)$$

At the end of the first stage, the internal temperature penetration depth of ice layer is

$$\delta_1(t_1) = \frac{3\lambda(T_m - T_0)}{h(T_w - T_m)} \quad (13)$$

(b) Stage 2: From the time when the temperature of the top of the ice layer reaches melting point until the temperature of ice layer bottom starts to rise

The ice layer begins to melt from the surface. The temperature at the melting interface H_2 is maintained at T_m. The temperature penetration depth continues to increase and $\delta_2(t_2) = H$. The temperature at the bottom of ice layer rises smoothly from T_0. Similarly, the equations about the temperature penetration depth $\delta_2(t)$ and the melting interface $H_2(t)$ are:

$$\frac{d\delta_2(t)}{dt} + \frac{dH_2(t)}{dt} = \frac{12a}{\delta_2(t) - H_2(t)} \quad (14)$$

$$\rho L_1 \frac{dH_2(t)}{dt} = -3\lambda \frac{T_m - T_0}{\delta_2(t) - H_2(t)} + h(T_w - T_m) \quad (15)$$

By solving the differential equations consisting of equations (14) and (15), the numerical solutions of $\delta_2(t)$ and $H_2(t)$ can be obtained. By solving $\delta_2(t_2) = H$, the end time t_2 of the second stage is calculated.

(c) Stage 3: From the time when the temperature at the bottom of the ice layer begins to rise to the end of melting

In this stage, the melting interface H_3 continues to increase. The temperature penetration depth has reached the maximum value H, and the temperature at the bottom of the ice layer is $T_n(t)$. When $t = t_3$, the melting interface H_3 reaches the bottom of the ice layer. At this time, the ice melting process within the effective heat transfer area of water column ends, and the ice melting time is t_3. Similarly, the equations for $T_n(t)$ and $H_3(t)$ are:

$$(H - H_3(t))\frac{dT_n(t)}{dt} + (T_m - T_n(t))\frac{dH_3(t)}{dt} = \frac{4a(T_m - T_n(t))}{H - H_3(t)} \quad (16)$$

$$\rho L_1 \frac{dH_3(t)}{dt} = -3\lambda \frac{T_m - T_n(t)}{H - H_3(t)} + h(T_w - T_m) \quad (17)$$

The numerical solutions of $T_n(t)$ and $H_3(t)$ are obtained by solving the differential equations of equations (16) and (17). By solving $H_3(t_3) = H$, the end time of the third stage, that is, the melting time t_3, is obtained.

At the same time, according to the relative size between $\delta_1(t_1)$ and ice thickness H, the melting process is divided into two cases. When the number $\mathrm{Bi} = hH/\lambda > 3(T_m\text{-}T_0)/(T_w\text{-}T_m)$, that is, the temperature penetration depth at the end of the first stage is smaller than the ice thickness H, the melting process is divided into the above three stages. When $\mathrm{Bi} \le 3(T_m\text{-}T_0)/(T_w\text{-}T_m)$, it indicates that the temperature penetration depth has reached the bottom of the ice layer at the end of the first stage, and there is no second stage in this case.

TABLE 1. Calculation parameters.

Parameter	Value	Unit	Parameter	Value	Unit
H	0.01	m	T_m	0	°C
T_0	-1	°C	T_w	40	°C
L	0.05	m	v	0.659	$10^6 m^2/s$
Pr	4.31	/	V_w	10	m/s
k	0.635	W/(m·°C)	λ	2.22	W/(m·°C)
ρ	917	kg/m^3	L_1	3.34	$10^5 J/kg$
a	1.15	$10^6 m^2/s$			

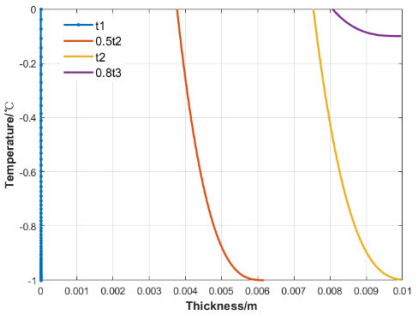

FIGURE 4. Temperature distribution inside the ice layer at different time.

The ice layer of $H = 0.01$ m is taken as an example to calculate and present the temperature distribution inside the ice layer at different time. Table 1 shows the parameters and ice/hydrothermal properties required for the calculation.

Fig. 4 shows the temperature distribution of ice layer in the thickness direction at t_1, 0.5 t_2, t_2 and 0.8 t_3. At the end of the first stage, the temperature penetration depth is about 8×10^{-6} m and the end time t_1 is 1.6×10^{-6} s. The second stage ends at $t_2 = 2.8$ s, at which time the temperature penetration depth reaches 0.01 m. The melting interface moves to 7.54×10^{-3} m, which means that the ice layer has melted by about 3/4 of the thickness by the end of the second stage. The third stage ends at $t_3 = 3.7$ s, at which time the melting interface moves to the bottom of the ice layer and the melting process ends.

Through the above heat transfer stages, the ice melting time within the effective heat transfer area of water column can be obtained, so the deicing time t of the single insulator is

$$t = S \times t_3 / S_w \quad (18)$$

where S_w is the effective heat transfer area of the water column on the ice layer surface, which can be calculated from the radial width x of water column, $S_w = \pi x^2/4$.

For insulator string, the total deicing time t_a is

$$t_a = n \cdot t \quad (19)$$

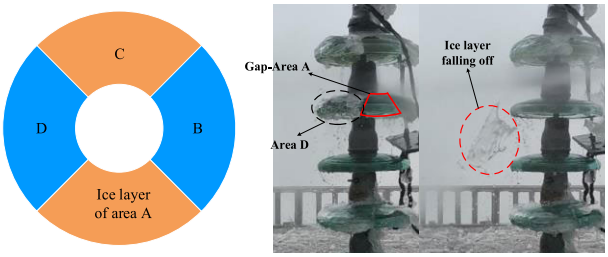

(a) The top view of ice layer (b) Ice layer shedding

FIGURE 5. The top view of insulator ice layer and phenomenon of ice layer falling off.

The total water consumption m_{water} is

$$m_{water} = 2.1d^2\sqrt{P} \cdot t_a \tag{20}$$

where d is the nozzle diameter, mm, P is the outlet pressure, MPa.

Deicing energy consumption E of hot water is

$$E = m_{water} c_{water} \left(T_{water} - T_i\right) \tag{21}$$

where c_{water} is the specific heat capacity of water, J/(kg· °C), T_{water} is the hot water temperature at the nozzle outlet, °C, T_i is the water temperature before heating, °C.

B. THE INFLUENCE OF MASS PROPORTION OF ICE LAYER SHEDDING

In the deicing experiment, it was found that the ice layer can usually form a "gap" by melting. The remaining small ice layers are not obstructed by the whole ice layer and directly washed away under the impact of the water jet. For example, Fig. 5 (a) shows the top view of the ice layer on the insulator surface. The ice layer is roughly divided into four areas. The ice layers in areas A and C are mainly removed through thermal melting due to the obstruction of the surrounding ice layers in areas B and D. After the ice in areas A and C is removed, the ice blocks in areas B and D will fall off under the impact force of water jet, as shown in Fig. 5 (b).

It is assumed that the mass proportion of shedding ice layer is X. Whether the ice falls off or not depends on whether the impact force of water jet is greater than the adhesion force between ice and insulator surface. Literature [31] measured the adhesion force between ice and glass plate at Xuefeng Mountain Natural Icing Test Base. It was found that when the ambient temperature is −5 °C or above, the adhesion force F_i of ice on the surface of glass plate is approximately linear with the ambient temperature T_0.

$$F_i = -0.197T_0 + 0.082 \tag{22}$$

where the uint of F_i is N/cm^2, the uint of $T_0$is °C.

Then the impact force F of water jet was measured. The test layout is shown in Fig. 6. The load sensor with resistance strain gauge as the conversion element was used to measure the impact force of water column. The sensor is vertically fixed on the bracket and the sensing plane is connected to a 23 cm × 23 cm force plate. A pressure gage is installed

(a) The test layout (b) Sensor force plate

FIGURE 6. Test layout of water jet impact force.

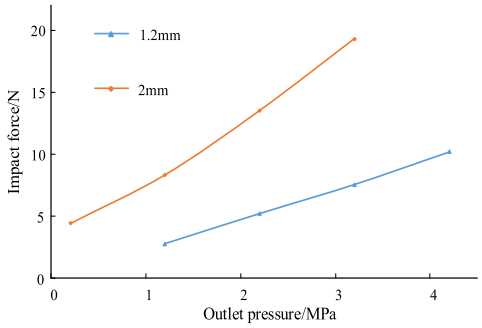

FIGURE 7. The impact force of water jet of two nozzles.

at the nozzle to simultaneously measure the outlet pressure corresponding to the impact force.

The measured impact force of 1.2 mm and 2 mm nozzle water jet at different outlet pressure at the distance of 2 m is shown in Fig. 7.

When the impact force of water jet is greater than the adhesion force of the remaining ice in areas B and D, the ice layer can shed as a whole, i.e. the condition of ice falling off is

$$F = F_i \cdot S_x \tag{23}$$

where S_X is the area of shedding ice layer, cm^2.

Therefore, the mass proportion X of the shedding ice is

$$X = S_x/S \tag{24}$$

The deicing time of hot water for insulator is

$$t = \frac{(1 - X)\, S}{S_w} \cdot t_3 \tag{25}$$

C. CALCULATION PROCESS OF HOT WATER DEICING FOR INSULATOR

According to the above physical process and calculation model, the calculation flow chart of the hot water deicing for insulator can be determined, as shown in Fig. 8.

D. VALIDATION OF CALCULATION MODEL FOR DEICING TIME OF HOT WATER

Taking LXY-120 glass insulator as the research object, the verification test of hot water deicing was carried out at Xuefeng mountain natural icing test base (test condition 1: nozzle diameter of 1.2 mm, ice weight of 0.95 kg/piece, wind speed of 3 m/s, temperature of −1 °C, outlet pressure of 3 MPa, deicing distance of 2 m; test condition 2: nozzle diameter of 2 mm, ice weight of 0.95 kg/piece, wind speed

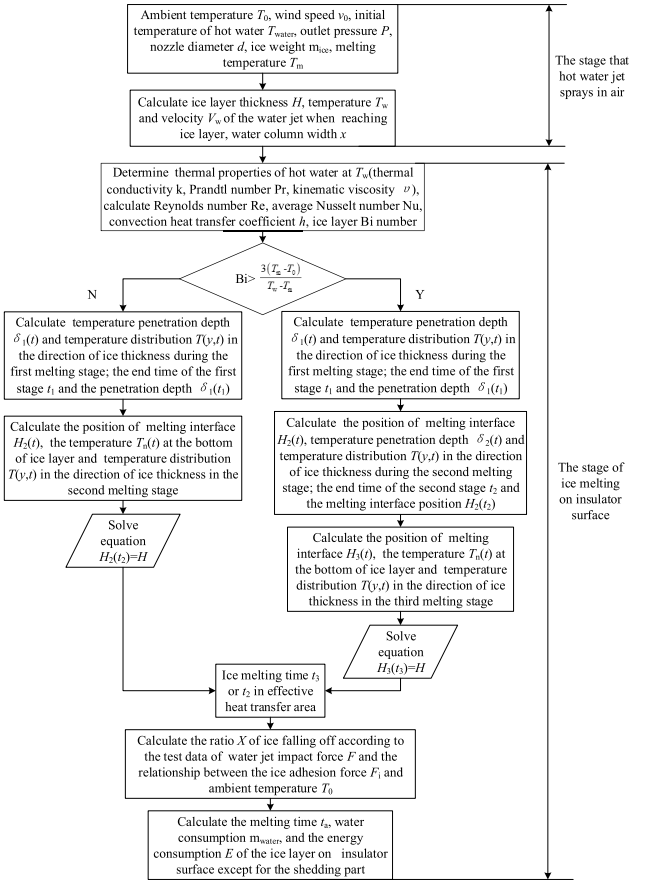

FIGURE 8. Calculation flow chart of hot water deicing for insulator.

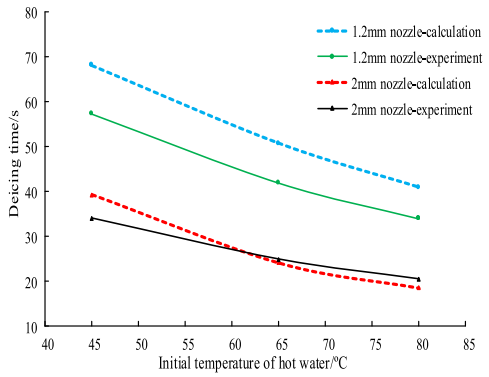

FIGURE 9. Comparison between calculated value and experimental value of deicing time.

of 0 m/s, temperature of −0.5 °C, outlet pressure of 1.6 MPa, deicing distance of 2 m). Three strings of insulators with the same icing condition were prepared for each test condition. The deicing experiment was carried out three times under each condition, and the average value was taken as the result of deicing time. According to the calculation process, the comparison between the calculated value of deicing time and the experimental result is shown in Fig. 9.

It can be seen from Fig. 9 that the calculated and experimental values decrease with the increase of the initial

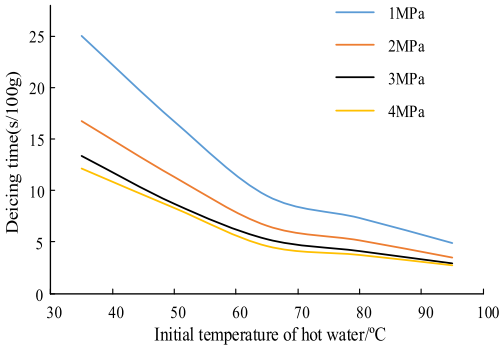

FIGURE 10. Relationship between deicing time and initial temperature of hot water.

temperature of hot water, and the regularity is the same. The error between the calculated value of 2 mm nozzle and the experimental value is less than 6%. The error between the calculated value of 1.2 mm nozzle and the experimental value is about 18%. The reason for the large error is that the field ambient wind speed is uncontrollable and dynamic and its average value is measured in the experiment, which is used for model calculation. Therefore, the hot water deicing model established in this paper can meet the engineering calculation requirement of hot water deicing time for insulator to some extent.

III. INFLUENCING FACTORS ON DEICING TIME OF HOT WATER FOR INSULATOR

In order to study the influence of initial temperature of hot water, outlet pressure and ice weight on deicing time, the above model (condition: 1.2 mm nozzle, environment temperature of −1 °C, wind speed of 3 m/s, deicing distance of 2 m, LXY-120 insulator) is used to calculate the deicing time under different initial temperature of hot water, outlet pressure and ice weight.

A. INFLUENCE OF INITIAL TEMPERATURE OF HOT WATER

When the mass of ice is 2 kg/piece, the relationship between the deicing time (per 100 g) and the initial temperature of hot water is obtained as shown in Fig. 10.

It can be seen from Fig. 10 that the deicing time (per 100 g) at each outlet pressure decreases with the increase of the initial temperature of hot water. The rate of change at low temperature is greater than that at high temperature. To be specific, when the water temperature is higher than about 65 °C, the decreasing trend of deicing time slows down, indicating that the benefit of raising the initial temperature of hot water in the middle and low temperature range to reduce the deicing time is better than that in the high temperature range.

B. INFLUENCE OF OUTLET PRESSURE

When the ice weight is 2 kg/piece, the deicing time (per 100 g) at different outlet pressure is calculated, as shown in Fig. 11.

The deicing time (per 100 g) at different initial water temperature decreases as the outlet pressure increases, but the reduction rate tends to be gentle. The reason for this

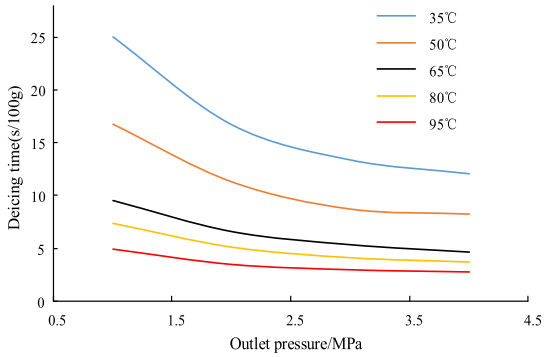

FIGURE 11. Relationship between deicing time and outlet pressure.

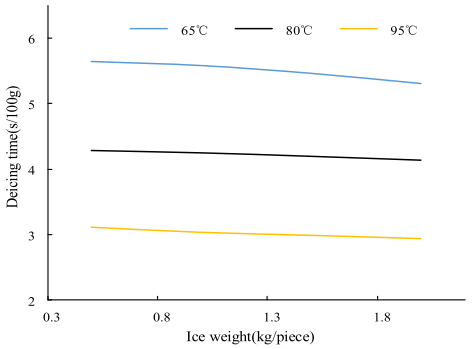

FIGURE 12. Relationship between deicing time and ice weight.

change trend is that the outlet pressure affects both the impact force and temperature of water jet. That is, increasing the outlet pressure will significantly increase the impact force at the same distance, as shown in Fig. 7, and the increasing impact force will increase the proportion of ice shedding and accelerate the deicing process. At the same time, according to the relationship between water jet temperature and outlet pressure in the first article of the series, the temperature of water jet decreases slightly with the increase of the outlet pressure. Therefore, under the comprehensive influence of the above two aspects, the reduction rate of deicing time decreases as the outlet pressure increases.

C. INFLUENCE OF ICE WEIGHT

The ice weight determines the amount of hot water. In order to prepare enough hot water for ice-covered insulator in the field operation, the relationship between deicing time and ice weight needs to be studied. When the ice weight of each insulator is between 0.5 and 2 kg, the deicing time (per 100 g) under different weight is obtained as shown in Fig. 12.

It can be seen from Fig. 12 that the deicing time (per 100 g) decreases slightly with the increase of ice weight. For example, when the ice weight increases from 0.5 kg/piece to 2 kg/piece, the deicing time (per 100 g) at initial water temperature of 65 °C, 80 °C and 95 °C reduces by 6.10%, 3.52% and 5.36% respectively. The influence of ice weight on the deicing time (per 100 g) is small. Therefore, the total deicing time of the insulator can be considered to rise linearly with the increase of ice weight.

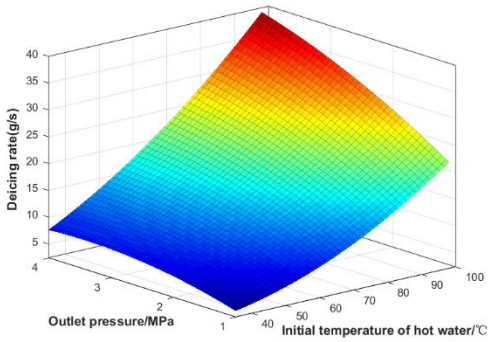

FIGURE 13. Distribution of deicing rate.

IV. OPTIMIZATION OF HOT WATER DEICING EFFICIENCY FOR INSULATOR

Hot water deicing efficiency needs to consider the effects of deicing time (i.e., deicing rate v_m: the ratio of ice weight to deicing time) and deicing energy consumption. In order to study the influence law of initial hot water temperature and outlet pressure on deicing efficiency, deicing rate (g/s) under different combinations of initial hot water temperature and outlet pressure is calculated using the above model (simulation condition: 1.2 mm nozzle, ambient temperature of −1 °C, wind speed of 3 m/s, ice weight of 2 kg/piece, deicing distance of 2 m), as shown in Fig. 13.

It can be seen from Fig. 13 that as the initial temperature of hot water T increases, the deicing rate v_m gradually increases. Besides, the deicing rate v_m gradually rises with the increase of outlet pressure P, but its increasing rate gradually decreases. The research results in literature [15] shows that the deicing rate of hot air satisfies the binary quadratic function with the initial temperature of hot air and outlet pressure. The fitting of Fig. 13 using the binary quadratic function gives

$$v_m = 0.00304T^2 - 0.3633P^2 + 0.04319TP - 0.12T + 2.262P + 0.2111 \quad (26)$$

The square of the fitting correlation coefficient is 0.99. The relationship between deicing rate of hot water and initial temperature of hot water, outlet pressure can also be expressed by a binary quadratic function.

Fig. 14 shows the distribution of deicing energy consumption (kJ/(100 g)) under different conditions. It can be seen from the figure that the relationship between energy consumption and temperature and pressure is more complicated. When the outlet pressure is constant, as the initial temperature of hot water T rises, the energy consumption E generally tends to decrease, which slows down between 65 °C and 80 °C. According to literature [15], the deicing energy consumption of hot air satisfies the binary quartic function with the initial temperature of hot air and outlet pressure. The binary quartic function is used to fit Fig. 14.

$$E = -0.0001061T^4 + 5.54 \times 10^{-5}T^3P + 0.00114T^2P^2 - 0.2045TP^2 - 0.01434T^2P + 0.02708T^3 - 2.637T^2 + 1.489TP + 10.69P^2 + 104T - 63.64P - 1239 \quad (27)$$

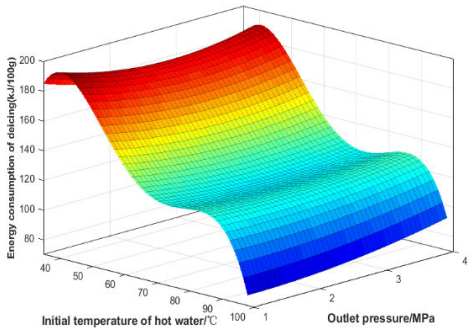

FIGURE 14. Distribution of deicing energy consumption.

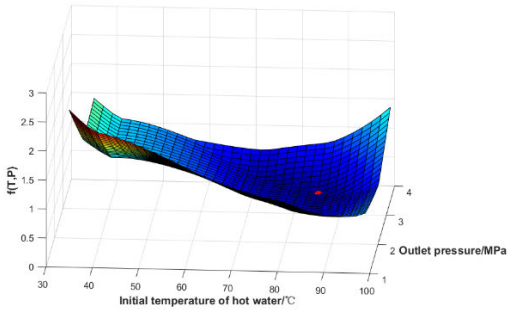

FIGURE 15. Distribution of objective function.

The square of the fitting correlation coefficient is 0.99. The relationship between deicing energy consumption of hot water and initial temperature of hot water, outlet pressure can also be expressed by a binary quartic function.

In order to obtain the maximum deicing efficiency, multi-objective optimization of deicing time and energy consumption is required. At the same time, since different initial water temperature and outlet pressure have different effects on reducing deicing time and energy consumption, that is, the slopes of the curves of deicing time and energy consumption reflect the contribution rate of temperature and pressure to improve the deicing efficiency. Therefore, the objective function for optimizing the initial hot water temperature and outlet pressure is constructed as follows,

$$\begin{aligned} &f\left(T,P\right)_{\min} \\ &= a\left(b\frac{t\left(v_{\mathrm{m}}\right)}{t\left(v_{\mathrm{m}}\right)_{\max}} + (1-b)\left(\left|\frac{\partial t\left(v_{\mathrm{m}}\right)}{\partial T}\right| + \left|\frac{\partial t\left(v_{\mathrm{m}}\right)}{\partial P}\right|\right)\right) \\ &\quad + (1-a)\left(b\frac{E}{E_{\max}} + (1-b)\left(\left|\frac{\partial E}{\partial T}\right| + \left|\frac{\partial E}{\partial P}\right|\right)\right) \end{aligned} \tag{28}$$

where $t(v_{\mathrm{m}})$ is the time to remove 100 g of ice, $t(v_{\mathrm{m}}) = 100/v_{\mathrm{m}}$; a is the weight of deicing time, (1-a) is the weight of energy consumption; b is the weight of the contribution rate of deicing time and energy consumption to deicing efficiency, (1-b) is the weight of the contribution rate of the initial water temperature and outlet pressure to deicing efficiency. According to the research of literature [15] and practical operation experience, $a = 0.8$ and $b = 0.8$ are taken. $t(v_{\mathrm{m}})/t(v_{\mathrm{m}})_{\max}$ is the ratio of deicing time to maximum deicing time under different conditions; $E/E_{\max}$ is the ratio of energy consumption to maximum deicing energy consumption under different conditions; $|\partial t(v_{\mathrm{m}})/\partial T|$ and $|\partial E/\partial T|$ are the partial derivatives of time and energy consumption to the initial temperature of hot water, respectively; $|\partial t(v_{\mathrm{m}})/\partial P|$ and $|\partial E/\partial P|$ are the partial derivatives of time and energy consumption to the outlet pressure, respectively.

The change intervals of independent variables T and P in this objective function are respectively

$$35 \le T \le 100, \quad 1 \le P \le 4 \tag{29}$$

The distribution of the objective function $f(T, P)$ is shown in Fig. 15. By solving the objective function, the result of $f(T, P)_{\min} = f(85.21, 3.35) = 0.305$ can be obtained, that is,

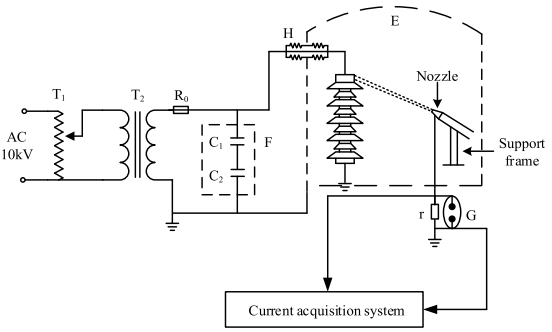

FIGURE 16. Schematic diagram of test circuit.

for the deicing condition of 1.2 mm nozzle, ambient temperature of −1 °C, wind speed of 3 m/s, ice weight of 2 kg/piece, and deicing distance of 2 m, when the initial temperature of hot water is between 35 °C and 100 °C and the outlet pressure is between 1 MPa and 4 MPa, the comprehensive deicing efficiency is the highest when the initial temperature of hot water and outlet pressures are 85.21 °C and 3.35 MPa respectively, as shown by the red marked point in Fig. 15.

V. SAFETY DISTANCE OF HOT WATER DEICING FOR LIVE INSULATOR

An experimental study was carried out on the water jet insulation characteristics of hot water deicing for operating insulator in 110 kV system. The influence of various factors on the leakage current was analyzed to obtain the minimum deicing distance under different outlet pressure and conductivity of deicing water.

A. EXPERIMENT EQUIPMENT AND METHOD

The test circuit and experiment layout are shown in Fig. 16 and Fig. 17 respectively [24], [25]. The high voltage pole is connected to the fitting of the first insulator. The measurement line is drawn from the metal part of nozzle, and the acquisition resistance enlarges the leakage current waveform by 100 times and converts it to voltage signal for measurement. Water column is adjusted to ensure effective contact between the water column and the high-pressure pole, that is, the leakage current is measured in the extreme case where the water jet directly contacts the high-pressure pole (at this time, the leakage current is the largest). The high-pressure

FIGURE 17. Experiment layout.

TABLE 2. The leakage current for 1 mm nozzle, 30 μS/cm and 1.5 MPa.

Distance (m)	0.7	0.85	1	1.5	2
Leakage current (mA)	0.496	0.426	0.388	0.280	0.187

water gun is fixed on the support frame. The applied test voltage is 110 kV. The temperature of hot water is 55 °C, and the lowest conductivity of the deicing water produced by industrial water system is 20.3 μS/cm at room temperature (20 °C).

B. EXPERIMENT RESULTS OF LEAKAGE CURRENT

(1) The leakage current of water jet decreases with the increase of distance. Taking 1 mm nozzle as an example, when the water conductivity is 30 μS/cm and outlet pressure is 1.5 MPa, the experiment results of leakage current are shown in Table 2.

According to the regulation of hot washing for electric power apparatus [24], the safe leakage current through water column should be less than 1 mA, indicating that under the above conductivity and outlet pressure, the water jet leakage current at a distance of 0.7-2 m meets safety requirement.

(2) Considering the general situation that the water source of on-site deicing operation may not provide the appropriate conductivity of deicing water, the leakage current under different deicing water conductivity (30-1800 μS/cm) and outlet pressure (0.5-1.5 MPa) was measured in this paper. For example, the leakage current distribution of 2 mm nozzle is shown in Fig. 18. It can be seen that the amplitude of leakage current changes significantly at large conductivity and close range, while at small conductivity and long distance, the change in leakage current tends to be mild.

(3) The leakage current rises with the increase of the outlet pressure. The smaller the distance or the higher the conductivity is, the faster the leakage current increases. For long water column or small conductivity, the effect of outlet pressure on the leakage current is not obvious, as shown in Fig. 19.

C. SAFETY DISTANCE OF DEICING

The relationship between the leakage current of water column in the live insulator washing and influencing factors such as distance was fitted as a polynomial in literature [25]. The leakage current of hot water deicing for live insulator is similar to the above situation. By fitting the leakage current of the nozzles with different diameters, the relationship between the leakage current I and distance L, the conductivity σ and outlet pressure P can be obtained, as shown in Fig. 18.

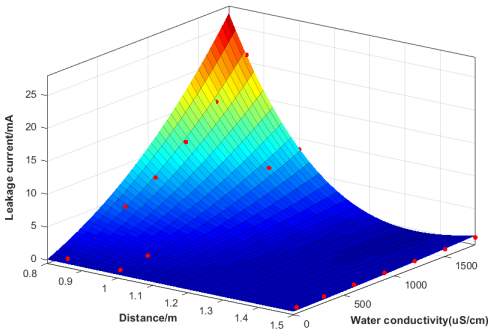

FIGURE 18. Distribution of leakage current.

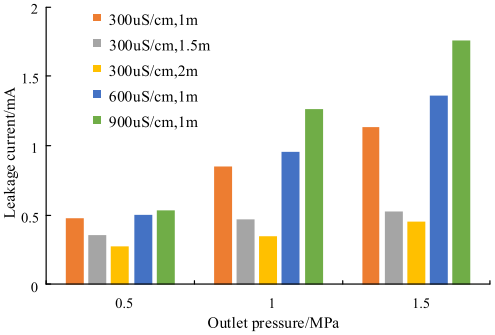

FIGURE 19. Leakage current under different outlet pressure.

TABLE 3. Minimum deicing distance/m.

Outlet pressure/ MPa	water conductivity (μS/cm)					
	300	600	900	1200	1500	1800
0.5	0.85	0.88	0.96	0.98	0.98	1.0
1.0	0.95	1.0	1.18	1.2	1.24	1.3
1.5	0.9	0.96	1.12	1.4	1.45	1.46

Since the safe leakage current of water jet should be less than 1 mA [24], the minimum deicing distance under different combinations of outlet pressure and water conductivity is calculated according to the fitting results of leakage current in this paper, as shown in Table 3.

The regulation of hot washing for electric power apparatus [24] stipulates that in 110 kV system, the safety distance using nozzles below 3 mm is not less than 1.5 m. It can be seen that the hot water deicing for insulator in 110 kV system can be carried out according to the safety distance of the existing regulation, and no special consideration is needed to its deicing distance.

VI. CONCLUSION

In this paper, the heat balance integral method is employed to solve the internal temperature of ice layer and the position of melting interface. At the same time, the influence of the proportion of the ice layer shedding caused by the impact force of water jet is considered, then the deicing time of hot water for insulator is calculated and analysed. With the aim of deicing efficiency, the initial temperature of hot water and outlet pressure are optimized. Finally, the leakage current test

of water jet under different working conditions is carried out. The following conclusions are drawn:

(1) The ice melting time is mainly distributed in the second and third stages. The phenomenon that ice layer falls off under the impact of water jet can accelerate the deicing process. The relative error between the calculated deicing time and the experimental value is small with the proportion of the ice layer shedding taken into consideration.

(2) The deicing time gradually decreases with the increase of the initial temperature of hot water and the outlet pressure, and tends to be gentle. The total deicing time of the whole insulator increases linearly as the ice weight increases.

(3) The deicing efficiency is determined by the deicing time (i.e., deicing rate) and deicing energy consumption. As the initial temperature of hot water increases, the deicing rate increases. As the outlet pressure increases, the deicing rate increases, but the rate of increase gradually decreases. The deicing energy consumption generally decreases with the increase of the initial temperature of hot water. For the deicing condition of 1.2 mm nozzle, ambient temperature of −1 °C, wind speed of 3 m/s, ice weight of 2 kg/piece, and deicing distance of 2 m, when the initial temperature of hot water is between 35 °C and 100 °C and the outlet pressure is between 1 MPa and 4 MPa, when the initial temperature of hot water and outlet pressures are 85.21 °C and 3.35 MPa respectively, the comprehensive deicing efficiency is the highest.

(4) The leakage current of water jet decreases as the distance increases. The shorter the distance or the higher the conductivity is, the more obviously the leakage current increases with outlet pressure. The hot water deicing for insulator in 110 kV system can be carried out according to the safety distance of the existing regulation, and no special consideration is needed to its deicing distance.

REFERENCES

[1] S. M. Ale-Emran and M. Farzaneh, "Flashover performance of ice-covered post insulators with booster sheds using experiments and partial arc modeling," *IEEE Trans. Dielectr. Electr. Insul.*, vol. 23, no. 2, pp. 979–986, Apr. 2016.

[2] F. Yin, M. Farzaneh, and X. Jiang, "Electrical characteristics of an energised conductor under various weather conditions," *High Voltage*, vol. 2, no. 2, pp. 102–109, Jun. 2017.

[3] M. Farzaneh and W. Chisholm, "50 years in icing performance of outdoor insulators," *IEEE Elect. Insul. Mag.*, vol. 30, no. 1, pp. 14–24, Jan. 2014.

[4] Q. Hu, S. Wang, L. Shu, X. Jiang, J. Liang, and G. Qiu, "Comparison of AC icing flashover performances of 220 kV composite insulators with different shed configurations," *IEEE Trans. Dielectr. Electr. Insul.*, vol. 23, no. 2, pp. 995–1004, Apr. 2016.

[5] Y. Hu, X. Jiang, L. Shu, Z. Zhang, Q. Hu, and J. Hu, "DC flashover performance of ice-covered insulators under complex ambient conditions," *IET Gener., Transmiss. Distrib.*, vol. 10, no. 10, pp. 2504–2511, Jul. 2016.

[6] M. Farzaneh, "Insulator flashover under icing conditions," *IEEE Trans. Dielectr. Electr. Insul.*, vol. 21, no. 5, pp. 1997–2011, Oct. 2014.

[7] S. Nacer, S.-A. El-Khider, C. Pierre, and L. Jack, "On the goodman heat-balance integral method for stefan like-problems: Further considerations and refinements," *Thermal Sci.*, vol. 13, no. 2, pp. 81–96, 2009.

[8] T. G. Myers, S. L. Mitchell, and G. Muchatibaya, "Unsteady contact melting of a rectangular cross-section material on a flat plate," *Phys. Fluids*, vol. 20, no. 10, Oct. 2008, Art. no. 103101.

[9] A. S. Wood, "A new look at the heat balance integral method," *Appl. Math. Model.*, vol. 25, no. 10, pp. 815–824, Oct. 2001.

[10] S. L. Mitchell and T. G. Myers, "Approximate solution methods for one-dimensional solidification from an incoming fluid," *Appl. Math. Comput.*, vol. 202, no. 1, pp. 311–326, Aug. 2008.

[11] C. D. Ho, H. M. Yeh, W. P. Wang, and J. K. Wang, "Cool thermal discharge obtained with air flowing over melting ice by complete removal of melt," *Int. Commun. Heat Mass Transf.*, vol. 27, no. 6, pp. 785–794, Aug. 2000.

[12] T. G. Myers, S. L. Mitchell, G. Muchatibaya, and M. Y. Myers, "A cubic heat balance integral method for one-dimensional melting of a finite thickness layer," *Int. J. Heat Mass Transf.*, vol. 50, nos. 25–26, pp. 5305–5317, Dec. 2007.

[13] J. Caldwell and C.-C. Chan, "Spherical solidification by the enthalpy method and the heat balance integral method," *Appl. Math. Model.*, vol. 24, no. 1, pp. 45–53, Jan. 2000.

[14] H.-S. Ren, "Application of the heat-balance integral to an inverse Stefan problem," *Int. J. Thermal Sci.*, vol. 46, no. 2, pp. 118–127, Feb. 2007.

[15] B. Li, L. He, Y. Liu, J. Luo, and G. Zhang, "Influences of key factors in hot-air deicing for live substation equipment," *Cold Regions Sci. Technol.*, vol. 160, pp. 89–96, Apr. 2019.

[16] L. Qi, X. Zhu, C. Zhu, F. Guo, G. Zhu, and S. Gu, "Deicing with Nd: YAG and CO_2 lasers," *Opt. Eng.*, vol. 49, no. 11, pp. 114301.1–114301.6, Nov. 2010.

[17] T. Xie, J. Dong, H. Chen, Y. Jiang, and Y. Yao, "Experiment investigation on deicing characteristics and energy efficiency using infrared ray as heat source," *Energy*, vol. 116, pp. 998–1005, Dec. 2016.

[18] K. Takahashi, N. Usami, T. Shibata, K. Goto, T. Uehara, H. Kondo, R. Ishikawa, and H. Saeki, "Experimental study on a deicing method using a water jet," in *Proc. IEEE TECHNO-OCEAN*, Kobe, Japan, Nov. 2004, pp. 1668–1673.

[19] Z. Guo, X. Long, Q. Liu, and M. Zhang, "Experimental study on water-jet deicing," in *Proc. Int. Symp. Fluid Machinery Fluid Eng. (ISFMFE)*, Wuhan, China, 2014, pp. 1–4.

[20] J. Hu, G. Shao, H. Cai, J. Fu, Z. Wen, and L. Wan, "Research on thermal electric deicing technology for substation equipment," *Electr. Power*, vol. 48, no. 6, pp. 85–90, Mar. 2015.

[21] J. Zhou, X. Xu, and W. Chu, "R&D of a new deicing device based on synthetically deicing techniques," *Appl. Mech. Mater.*, vol. 372, pp. 381–386, May 2013.

[22] Z. Zhu, X. Zhang, Q. Wang, and C. Wei, "Research and experiment of thermal water deicing device," *Trans. Can. Soc. Mech. Eng.*, vol. 39, no. 4, pp. 783–788, 2015.

[23] D. Dai, "Research on road deicing vehicle with combined thermal water jet device and machinery," Dept. Mech. Eng., Huazhong Univ. Sci. Technol., Wuhan, China, 2015.

[24] *Regulation of Hot Washing for Electric Power Apparatus*, CEC Standard 13395, 2008.

[25] S. Huang, "Research on hot washing technology for 500 kV substation insulators," Ph.D. dissertation, Dept. Elect. Eng., Wuhan Univ, Wuhan, China, 2014.

[26] J. P. Holman, *Heat Transfer*. Beijing, China: China Machine Press, 2011.

[27] F. P. Incropera and D. P. Dewitt, *Fundamental of Heat and Mass Transfer*. New York, NY, USA: Wiley, 2007.

[28] H. Martin, "Heat and mass transfer between impinging gas jets and solid surfaces," *Adv. Heat Transf.*, vol. 13, no. 1, pp. 1–60, 1977.

[29] H. G. Landau, "Heat conduction in a melting solid," *Quart. Appl. Math.*, vol. 8, no. 1, pp. 81–94, Nov. 1950.

[30] S. J. Citron, "Heat conduction in a melting slab," *J. Aerosp. Sci.*, vol. 27, no. 3, pp. 219–228, Sep. 1960.

[31] M. Bi, X.-L. Jiang, Y.-F. Chao, L. Chen, D.-H. Xiao, and W. Liu "Adhesion strength and its influence analysis of natural ice on various substrates," *High Voltage Eng.*, vol. 37, no. 4, pp. 1050–1056, Apr. 2011.

ZHANG ZHIJIN was born in Fujian, China, in 1976. He received the B.Sc., M.Sc., and Ph.D. degrees from Chongqing University, Chongqing, China, in 1999, 2002, and 2007, respectively. He is currently a Professor with the College of Electrical Engineering, Chongqing University. He has authored or coauthored several technical articles. His main research interests include high voltage, external insulation, numerical modeling, and simulation.

YANG SHENGHUAN was born in Sichuan, China, in 1995. He graduated from Chongqing University, Chongqing, China, in 2017. He is currently pursuing the M.S. degree with the School of Electrical Engineering, Chongqing University. His main research interests include high-voltage engineering, external insulation, and transmission-line icing.

JIANG XINGLIANG (Senior Member, IEEE) was born in Hunan, China, in 1961. He graduated from Hunan University, in 1982, and received the M.Sc. and Ph.D. degrees from Chongqing University, Chongqing, China, in 1988 and 1997, respectively. His employment experience includes the Shaoyang Glass Plant, Shaoyang, Hunan, the Wuhan High Voltage Research Institute, Wuhan, Hubei, and the College of Electrical Engineering, Chongqing University. He has published his first monograph—*Transmission Line's Icing and Protection*, in 2001, and has published over 120 articles about his professional work. His special fields of interest include high-voltage external insulation and transmission line's icing and protection. He received the First-class Reward of National Technology Improvements, in 2013, the Second-class Reward for Science and Technology Advancement from the Ministry of Power, in 1995, Beijing Government, in 1998, and the Ministry of Education, in 1991 and 2001, the First-class Reward for Science and Technology Advancement from the Ministry of Power, in 2004, the Third-class Reward for Science and Technology Advancement from the Ministry of Power, in 2005, the Second-class Reward for Science and Technology Advancement from the Ministry of Technology, in 2005, the First-class Reward for Science and Technology Advancement from the Ministry of Education, in 2007, and the First-class Reward for Science and Technology Advancement from Chongqing City, in 2007.

MA XIAOHONG was born in Ningxia, China, in 1978. She received the B.Sc. degree from North China Electric Power University, Baoding, China, in 2001, and the M.Sc. degree from Shanghai Jiao Tong University, Shanghai, China, in 2005. She is currently an Associate Senior Engineer with the High Voltage Department, Electric Power Research Institute, Guizhou Power Grid Company Ltd., Guiyang, China. Her main research interests include high voltage, external insulation, and anti-ice technology.

HUANG HUAN was born in Hunan, China, in 1978. She received the M.Sc. degree from Chongqing University, Chongqing, China, in 2008. She is currently an Associate Senior Engineer with the High Voltage Department, Electric Power Research Institute, Guizhou Power Grid Company Ltd., Guiyang, China. Her main research interests include high voltage, external insulation, and anti-ice technology.

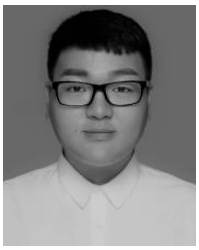

PANG GUOHUI was born in Henan, China, in 1996. He graduated from Chongqing University, Chongqing, China, in 2019, where he is currently pursuing the M.S. degree with the School of Electrical Engineering. His main research interests include high-voltage engineering and external insulation.

JI YAQING was born in Hebei, China, in 1998. She graduated from North China Electric Power University, Hebei, in 2019. She is currently pursuing the M.S. degree with the School of Electrical Engineering, Chongqing University, Chongqing, China. Her main research interests include high-voltage engineering and external insulation.

DONG KAI was born in Liaoning, China, in 1996. He graduated from China Three Gorges University, Hubei, China, in 2019. He is currently pursuing the M.S. degree with the School of Electrical Engineering, Chongqing University, Chongqing, China. His main research interests include high-voltage engineering and external insulation.